CORE
Provided by NASA Technical Reports Server
Metadata, citation and similar papers at core.ac.uk

N 70 25608
NASA CR 109526
T-70-18039

THIRD QUARTERLY REPORT:
SOLAR CELL PERFORMANCE
MATHEMATICAL MODEL

Prepared for the
California Institute of Technology
Jet Propulsion Laboratory

JPL CONTRACT 952548

CASE FILE
COPY

By
M. J. Barrett, M. B. Hornstein, and R. H. Stroud

Exotech Incorporated
525 School Street, S.W.
Washington, D.C. 20024

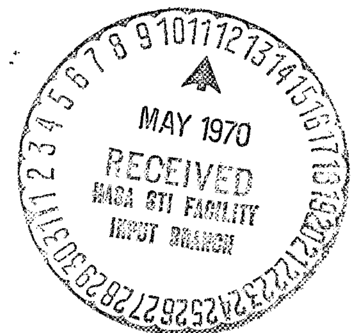

March 15, 1970

TR-SR708

THIRD QUARTERLY REPORT:
SOLAR CELL PERFORMANCE
MATHEMATICAL MODEL

Prepared for the
California Institute of Technology
Jet Propulsion Laboratory

By
M. J. Barrett, M. B. Hornstein, and R. H. Stroud

Exotech Incorporated
525 School Street, S.W.
Washington, D.C. 20024

March 15, 1970

This work was performed for the Jet Propulsion Laboratory, California Institute of Technology, as sponsored by the National Aeronautics and Space Administration under Contract NAS7-100.

This report contains information prepared by Exotech Incorporated under JPL subcontract. Its content is not necessarily endorsed by the Jet Propulsion Laboratory, California Institute of Technology, or the National Aeronautics and Space Administration.

ABSTRACT

Results of the third three months of an effort to prepare a computer program for silicon solar cell performance in the space environment are reported. The previous mathematical model has been expanded to include additional constructional and environmental parameters. A description of the computer program in its present form is given. Numerical and graphical results of computations are also provided.

TABLE OF CONTENTS

Section	Page
INTRODUCTION.	1.
I. EXTENSIONS OF PREVIOUS ANALYSIS.	2.
A. Summary.	2.
B. Surface Region	4.
C. Temperature Effects.	10.
D. Illumination Effects	13.
E. Proton Irradiation	17.
II. PROGRAM MODULE DESCRIPTIONS.	18.
A. Subroutine ABSCIS.	20.
B. Subroutine LIGHT	20.
C. Subroutine COVER	20.
D. Subroutines PROTON and DAMAGE.	21.
E. Subroutine ELECT	21.
F. Subroutine ROOT.	22.
G. Subroutine TRAP.	22.
H. Subroutine CURVE	23.
III. CONCLUSIONS AND RECOMMENDATIONS.	25.
IV. NEW TECHNOLOGY	26.
REFERENCES.	27.

INTRODUCTION

This is the third quarterly report on a one year program to provide computational methods for prediction of solar cell performance in a natural radiation environment. It covers work performed during the period 1 December 1969 through 28 February 1970. The model for the theoretical calculation of solar cell performance under space conditions, prepared under contract 952246 with the Jet Propulsion Laboratory, is the basis of this work.

In previous quarters of this program, the model was refined and used, with the aid of a computer, to examine consequences of various environmental factors. Numerical values of electrical parameters as functions of cell dimensions and environmental conditions were presented.

The work reported herein consists of preparation leading to the complete computer program that includes the final forms of the analytical effort discussed previously. Section I presents some of the recent choices that were made leading to various equations used in the program. Section II presents a detailed description of the modules of the program.

I. EXTENSIONS OF PREVIOUS ANALYSIS

A. Summary

The computer program for solar cell performance, begun earlier during the course of this contract, and reported in the Second Quarterly Report, was expanded to include additional calculations. These calculations permit a determination of the effects of combined radiations. The effect of isotropic fluences of protons and electrons of assorted energies can be handled simultaneously.

A second major extension of the program permitted consideration of the dopant profile forming the junction. This extensive calculation was necessary for the determination of the surface contribution to the electrical parameters, particularly the photovoltaic current density. In order to simplify the program, values for the surface contribution J_n to the photovoltaic current density were obtained under varying conditions of junction depth, temperature, illumination and radiation damage. An empirical equation was then obtained which related J_n to those factors. The equation is explained in Section I B.

More exact approximations for the derivatives used in the calculation of minority carrier concentrations were developed. These changes are simpler to explain if only the base region is considered. The argument is also valid in the surface region, but there it is complicated by the fact that the impurity concentration and the diffusion coefficient are variables. The derivation can be demonstrated with Figure 1 and the variable mesh scheme described in the First Quarterly Report.

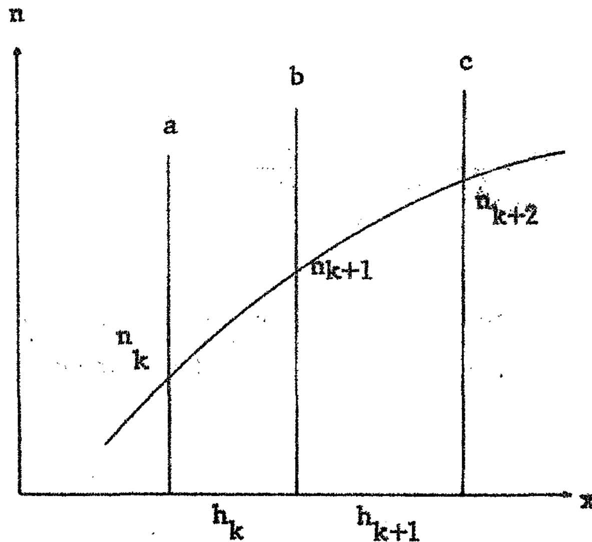

Figure 1. Construction of variable mesh h_k to approximate the curve $n(x)$ at points n_k

The slope of the curve between a and b, and between b and c are approximated as constants. The first derivative of the curve, evaluated at b, is taken as the average of the slope on either side of b, i. e.

$$\left.\frac{\Delta n}{\Delta x}\right|_b = \frac{1}{2}\left(\frac{n_{k+2} - n_{k+1}}{h_{k+1}} + \frac{n_{k+1} - n_k}{h_k}\right)$$

$$= \frac{n_{k+2}\, h_k + n_{k+1}\left(h_{k+1} - h_k\right) - n_k\, h_{k+1}}{2h_k\, h_{k+1}} \qquad (1)$$

The second derivative is derived as described previously. It is then

$$\left.\frac{\Delta^2 n}{\Delta x^2}\right|_b = \frac{n_{k+2}\, h_k - n_{k+1}\left(h_k + h_{k+1}\right) + n_k\, h_{k+1}}{h_k\, h_{k+1}\left(h_k + h_{k+1}\right)} \tag{2}$$

Using equation 1 and 2 in the continuity equation with the field terms eliminated, the minority carrier concentration can be found from

$$n_{k+2}\left[\frac{2}{h_{k+1}\left(h_k + h_{k+1}\right)}\right] = n_{k+1}\left[\left(\frac{2}{h_k\, h_{k+1}} + \frac{1}{L^2_{k+1}}\right)\right] - n_k\left[\frac{2}{h_k\left(h_k + h_{k+1}\right)}\right] - \frac{G_{k+1}}{D} \tag{3}$$

B. Surface Region

The surface region of a solar cell, typically only 0.2 to 0.5 microns thick, must contribute a minor amount to the photovoltaic current. Calculation of this contribution with the techniques used for the base region is complicated by several factors. To begin with, the normal process of junction formation by in-diffusion of n-type impurity atoms is recognized to result in a complemetary error function type of distribution of donor atoms [1]. The concentration $N(x)$ is related to the surface concentration $N(0)$ by the temperature-dependent atom diffusion coefficient D and the process time t by

$$N(x) = N(0)\ \mathrm{erfc}\left(x/\sqrt{4Dt}\right) \tag{4}$$

The particulars of this process would generally be unavailable to users of our code, so that some estimates are useful. A typical value of N(0) appears to be 10^{20} atoms / cm^3. The product Dt, if unknown from the process, can be calculated if the junction depth is known. At the junction, N(x) must equal the impurity concentration of the base material.

The code uses a polynomial approximation to the error function [2]

$$\text{erfc}\left(y\right) = \left(c_4\ n^4 + c_3\ n^3 + c_2\ n^2 + c_1\ n\right)\frac{2}{\sqrt{\pi}}\ e^{-y^2} \qquad (5)$$

where:

$n = \dfrac{1}{1 + 0.381965\,y}$

$c_1 = 0.12771538$

$c_2 = 0.54107939$

$c_3 = 0.53859539$

$c_4 = 0.75602755$

$y = x / \sqrt{4Dt}$

The non-uniform impurity concentration over the surface region also causes variation in the minority carrier diffusion coefficient D_p. The term D_p is the diffusion coefficient for holes and should not be confused with D, the atomic diffusion coefficient used above. Since D_p does not change uniformly with concentration, the variation with impurity concentration

shown by Conwell [3] is used. Since no simple equation will fit the entire curve, it was decided that the best approach was a series of empirical equations. These are:

$$
\begin{array}{lll}
\text{for} \quad N < 10^{15} & D_p = 13.0 & \text{(a)} \\
10^{15} < N < 10^{16} & D_p = 52.0-2.6 \ \log N & \text{(b)} \\
10^{16} < N < 10^{17} & D_p = 56.16-2.86 \ \log N & \text{(c)} \\
10^{17} < N < 10^{18} & D_p = 82.86-4.42 \ \log N & \text{(d)} \\
10^{18} < N < 10^{19} & D_p = 41.28-2.1 \ \log N & \text{(e)} \\
N < 10^{19} & D_p = 1.0 & \text{(f)}
\end{array}
\tag{6}
$$

For the surface region, where the field is not negligible, the continuity equation is

$$G - \frac{p}{\tau_p} + p_n \mu_p \frac{dE}{dx} - \mu_p E \frac{dp_n}{dx} + D_p \frac{d^2 p_n}{dx^2} = 0 \tag{7}$$

where: p = concentration of holes

τ_p = lifetime of holes

μ_p = mobility of holes

E = field due to impurity gradient $= - \frac{kT}{q} \frac{1}{N} \frac{dN}{dx}$

Using equations 4, 5, 6 and 7, we solve the continuity equation on the computer by putting it in the form of a difference equation, in the manner demonstrated in the previous reports.

$$p_{k+2}\left[\frac{2}{h_{k+1}\left(h_k+h_{k+1}\right)}+\frac{1}{2h_{k+1}}\frac{dN}{dx}\frac{1}{N_{k+1}}\left(\frac{dD_p}{dx}\frac{1}{D_{p(k+1)}}+1\right)\right]=p_{k+1}\left[\frac{2}{h_k h_{k+1}}+\right.$$

$$\left.\frac{\left(h_k-h_{k+1}\right)\frac{dN}{dx}\frac{1}{N_{k+1}}\left(\frac{dD_p}{dx}\frac{1}{D_{p(k+1)}}+1\right)}{2\left\{2h_k h_{k+1}-\frac{1}{N_{k+1}}\left[\frac{d^2N}{dx^2}+\left(\frac{dN}{dx}\right)^2\frac{1}{N_{k+1}}\left(\frac{dD_p}{dx}\frac{1}{D_{p(k+1)}}-1\right)\right]\right\}}+\frac{1}{L^2_{k+1}}\right]$$

$$-p_k\left[\frac{2}{h_k\left(h_k+h_{k+1}\right)}-\frac{1}{2h_k}\frac{dN}{dx}\frac{1}{N_{k+1}}\left(\frac{dD_p}{dx}\frac{1}{D_{p(k+1)}}+1\right)\right]-\frac{G_{k+1}}{D_{p(k+1)}} \qquad (8)$$

In the base region, where $\frac{dN}{dx}$ and $\frac{dD}{dx}$ vanish, equation (8) is reduced to equation (3) by substituting "n" (electron) for each "p" (hole) term.

The inclusion of these equations in the final program would unnecessarily lengthen the computing time. The routines for the surface region, therefore, were run separately, with varying temperature, junction depth, radiation and illumination intensity. The variation of the surface contribution to the current density J_n with temperature was curve-fitted as

$$J_n = 9.89 \times 10^{-3}\, T + 3.960 \text{ mA/cm}^2 \qquad (9)$$

The maximum deviation in the range 250° to 350°K is 0.19% in current density.

J_n vs. the junction depth x_j (in microns) at 300°K is plotted in Figure 2. A maximum deviation of 1.1% for junction depths of 0.3 to 1.0 microns is obtained with use of the the expression

$$J_n = 4.182 \ln x_j + 9.88 \text{ mA/cm}^2 \qquad (10)$$

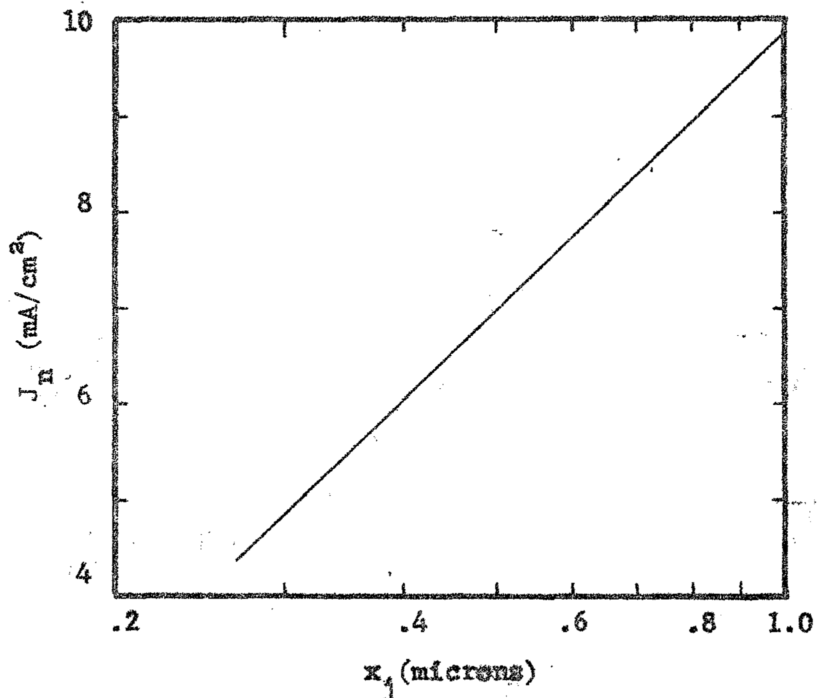

Figure 2. Variation of surface current density with junction depth. (theoretical)

In order to generalize the radiation effect, J_n was plotted as a function of the diffusion length L_n (in microns) of electrons in the first increment of the base region. The assumption here is that L_n, measured in the base region near the junction, measures the amount of radiation exposure the surface region has received. For the thickness of practical solar cell surface regions, the damage is uniform and this value of L_n is an indicator of the exposure. The values calculated are shown in Figure 3. The empirical equation, which has a maximum deviation of 2.2% for L_n greater than .12 microns, is

$$J_n = J_{no} - e^{-5.353\, L_n} \quad \text{mA/cm}^2 \tag{11}$$

where: J_{no}, the initial surface current density may be taken as 6.94 mA/cm^2 for x_j = 0.5 μ, T = 300°K, and U = 140 mW/cm^2.

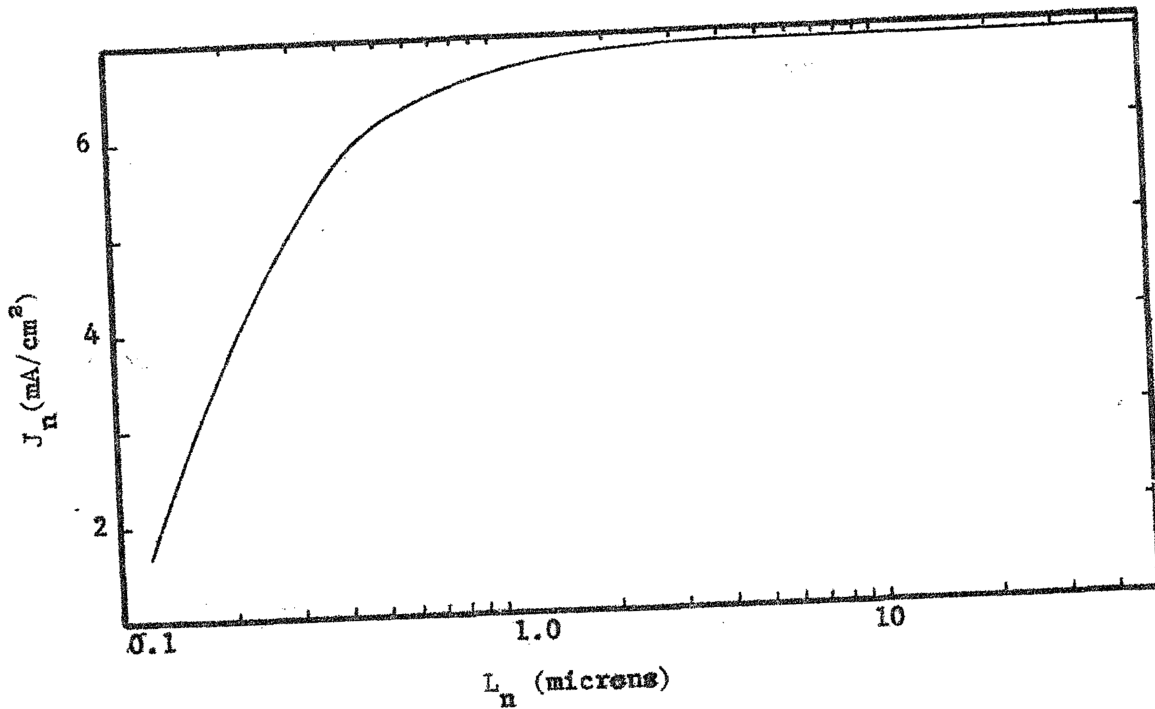

Figure 3. Variation of surface current density with electron diffusion length at h_1 (from computer program)

Since the light generated current is directly proportional to the illumination intensity

$$J_n = J_{no} \ (U/140) \ mA/cm^2 \tag{12}$$

These equations have been combined into a single empirical formula for use in the program. The expression is

$$J_n = (0.01408 + 0.005956 \ \ln x_j - 0.01411e^{-5.353 \ L_n}) \ (T + 400) \ (U/140) \ mA/cm^2 \tag{13}$$

Use of this expression to estimate the surface region contribution to the photovoltaic current permits us to bypass a more involved calculation such as used for the major contribution by the base region.

C. Temperature Effects

The variation of the light generated current I_L with temperature was discussed briefly in the Second Quarterly Report. During this quarter, the theory behind this dependence was examined in greater depth. The theory shows that the change in I_L is caused by changes in three of its parameters: the light absorption coefficient α, the minority carrier diffusion coefficient D_p (or D_n) and the lifetime τ. The first term is shown by Macfarlane and Roberts [4] to be equal to

$$\alpha = A\left[\frac{1}{1-e^{-\theta/T}}\left(\frac{h\nu - E_g - k\theta}{h\nu}\right)^2 + \frac{1}{e^{\theta/T}-1}\left(\frac{h\nu - E_g + k\theta}{h\nu}\right)^2\right] \tag{14}$$

where: A is a constant

$\theta = 600^{\circ}K$

$h\nu$ = energy of incident light

E_g = energy gap of the semiconductor

k = Boltzmann's constant

Since E_g varies very slowly with temperature (-0.00013 ev/$^{\circ}$C for silicon [5]) the quantities $\left[(h\nu - E_g - k\theta)/h\nu\right]^2$ and $\left[(h\nu - E_g + k\theta)/h\nu\right]^2$ can be considered constant for each wavelength, making α proportional to $\left[1/(1-e^{-\theta/T}) + 1/(e^{\theta/T}-1)\right]$. At $\lambda = 1.1\ \mu$, where $h\nu$ is very close to E_g, the value of α changes only 7% between 250°K and 300°K. Since light in this region of the spectrum contributes only a small number of carriers, the effect may be neglected. At lower wavelengths the variation is even smaller. If the above quantity is designated as f, and (f-1) is plotted as a function of θ/T, as in Figure 4, a straight line results. The equation which fits this line with a maximum deviation of less than 1%, is

$$\ln (f - 1) = 1.201 - 1.171\ \frac{\theta}{T} \tag{15}$$

From equation (15), the relationship between α and T can be shown to be

$$\alpha\ (\lambda,T) = \alpha\ (\lambda,300)\ \frac{3.323e^{-702.6/T}+1}{1.319} \tag{16}$$

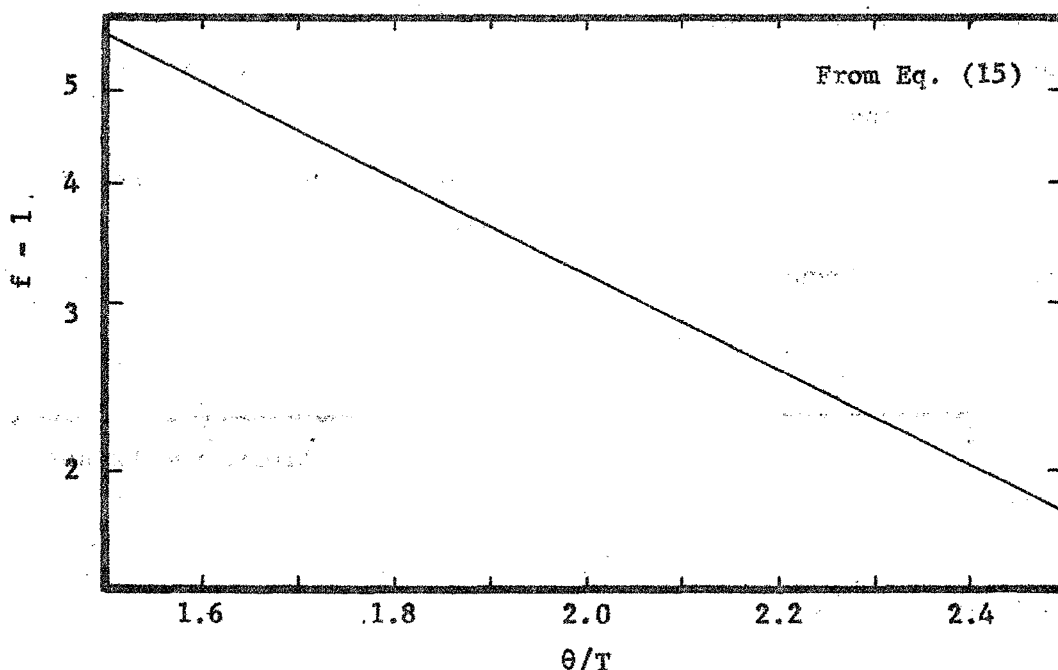

Figure 4. Relationship of absorbtion coefficient to temperature.

The effect of temperature on the diffusion coefficient in silicon may be determined from measured values of the temperature - mobility relationship. The measurements [6] show that for electrons the mobility varies as $T^{-2.6}$, and that for holes it varies as $T^{-2.7}$. By use of the Einstein relationship, D_n varies as $T^{-1.6}$ and D_p varies as $T^{-1.7}$.

The effect of temperature on the minority carrier lifetime τ has not been determined theoretically. It is composed of many factors, most of which depend upon the specific processing that the cell has been subjected to. Each of the process steps changes the number, type, and energy level of the trapping centers that determine the lifetime.

The temperature dependence of many types of traps has not been described in the literature. It was therefore necessary to assume a relationship that is consistent with experimental results. Knowing the temperature dependences of α and D, different functions for τ could be tried. If τ is taken as proportional to $T^{6.5}$, the temperature coefficient of I_L in the region about 300°K is 0.05%/°C, which is consistent with the photovoltaic current measurements given by Reynard [7] and others.

Figure 5 shows the variation of the open current voltage V_{oc} with temperature and compares the results with the experimental data given by Reynard.[7]

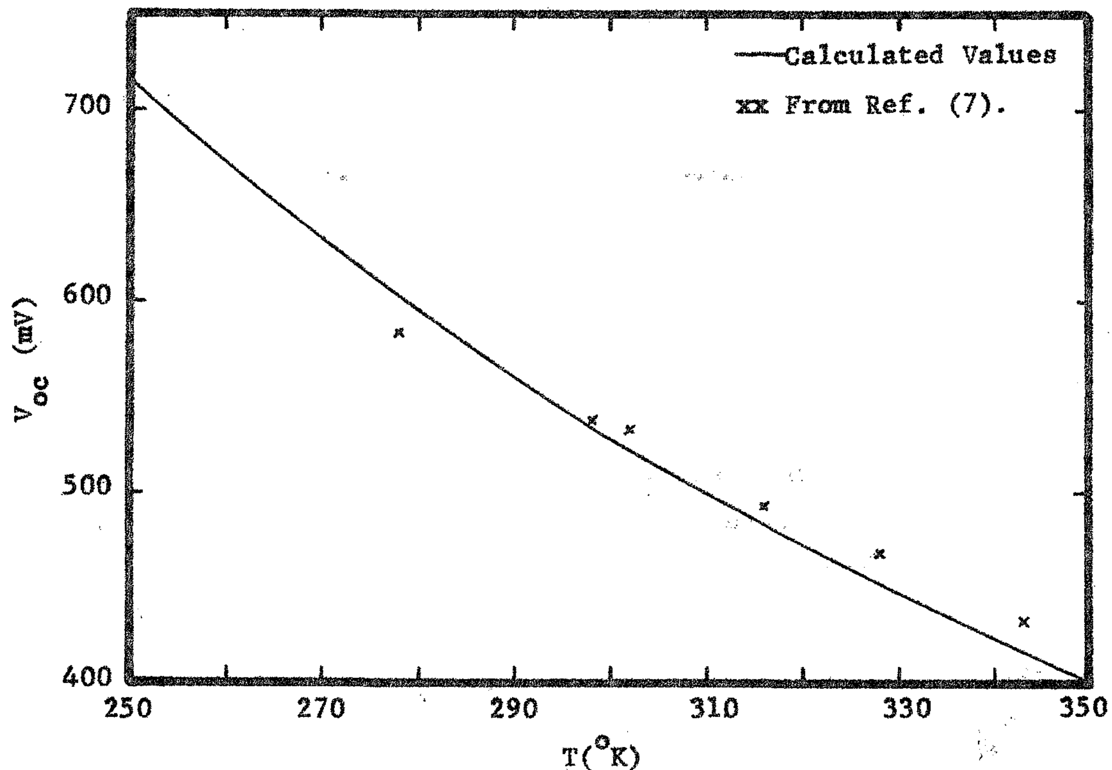

Figure 5. Variation of open circuit voltage with temperature

D. Illumination Effects

Information relating the diode saturation current to illumination is not available from theory or direct measurements, but can best be calculated from experimental data on the open circuit voltage V_{oc}, since the photovoltaic current is proportional to illumination. According to Ritchie and Sandstrom [8], V_{oc} increases at a rate of 0.2 mV/mW/cm² with increasing illumination intensity U. I_o can be calculated from this using the standard solar cell equation. If I_o is plotted against $\ln U$, as in Figure 6, the curve can be approximated by a straight line:

$$I_o = 0.0627 \ln U - .134 \ \mu A \tag{17}$$

The maximum deviation in I_o between the line and the calculated values is 2.1% in the range of 90-190 mW/cm².

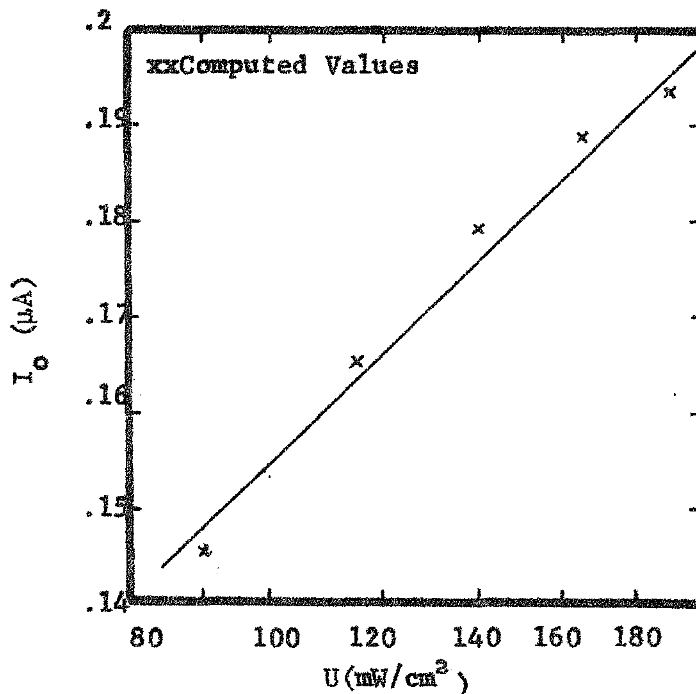

Figure 6. Variation of diode current with illumination intensity.

In Figure 7 a comparison is made between the I-V curves generated by the program and those reported by Ritchie and Sandstrom [8]. Since only the cell thickness and temperature are known, assumptions had to be made as to the junction depth and V_o. Using x_j equal to 1 micron and V_o equal to 45mV, made I_{sc} and V_{oc} comparable to the measured values.

The variation of maximum power P_{max} with illumination was also examined. The results, shown in Figure 8, indicate that P_{max} varies linearly with U.

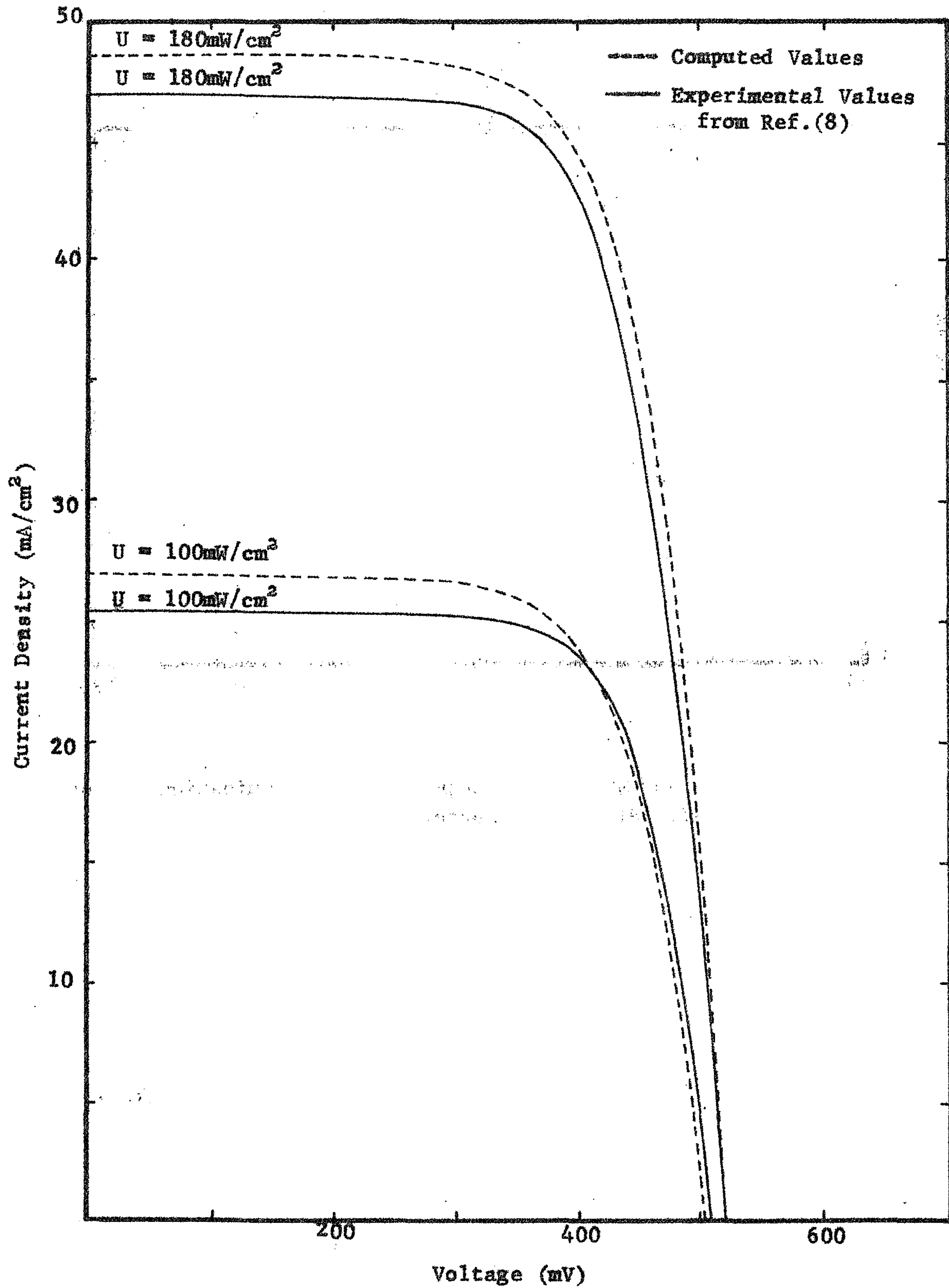

Figure 7. Comparison of calculated I-V curves with experiment (Experimental values of I reported for a 4 cm^2 cell, have been divided by 4.)

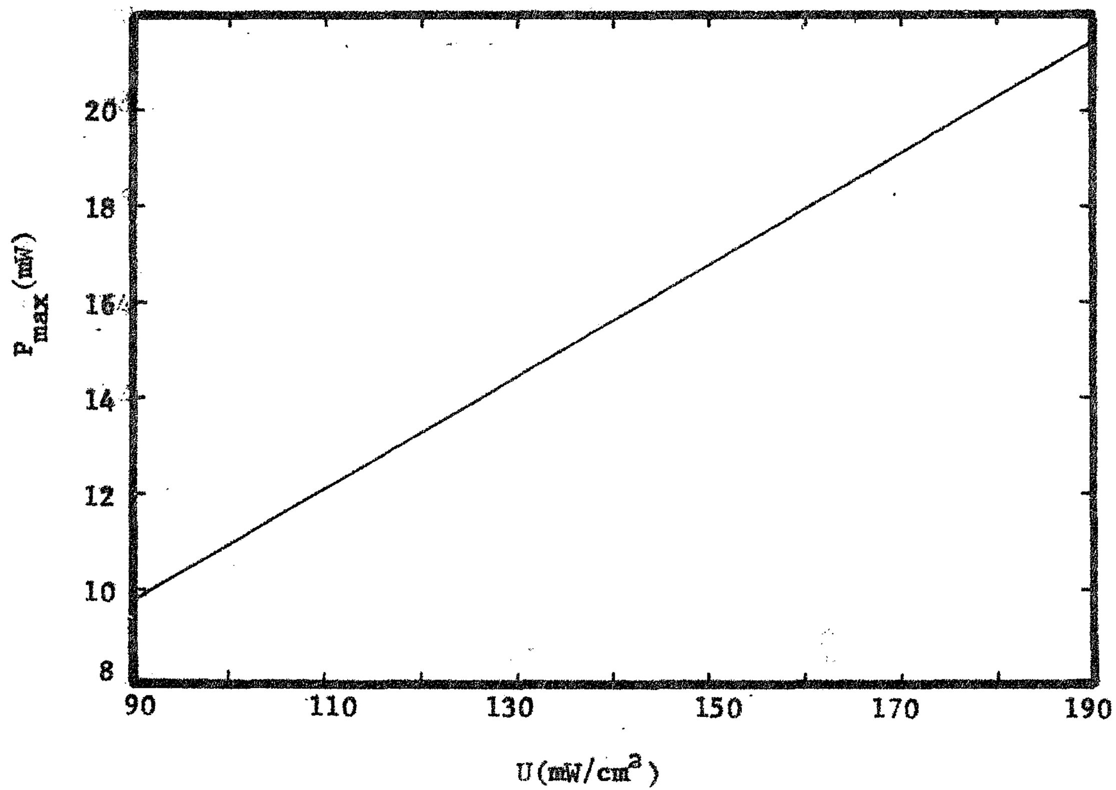

Figure 8. Variation of maximum power with illumination intensity. (calculated via computer program)

E. Proton Irradiation

In the Second Quarterly Report, the importance of the surface region in determining the rate of degradation of I_{sc} with low-energy proton irradiation was discussed, but correlation between the program results and experimental data was not possible at that time. The use of the program including the diffused surface region, produced an I_L vs. Φ curve closer to the experimental results than any previously obtained. As mentioned in earlier reports, the value of the damage coefficient K for low energy protons is uncertain. If K is taken to be $\frac{1}{3}$ of the previously used value, the rate of degradation of I_L is almost identical to the rate measured by Statler and Curtin [9] up to $\Phi = 2 \times 10^{13}$ p/cm^2, as can be seen in Figure 9. Since space applications are seldom concerned with fluences greater than 10^{13} p/cm^2, no further attempt was made to fit the data at higher fluences. More experimental effort in this area is clearly warranted.

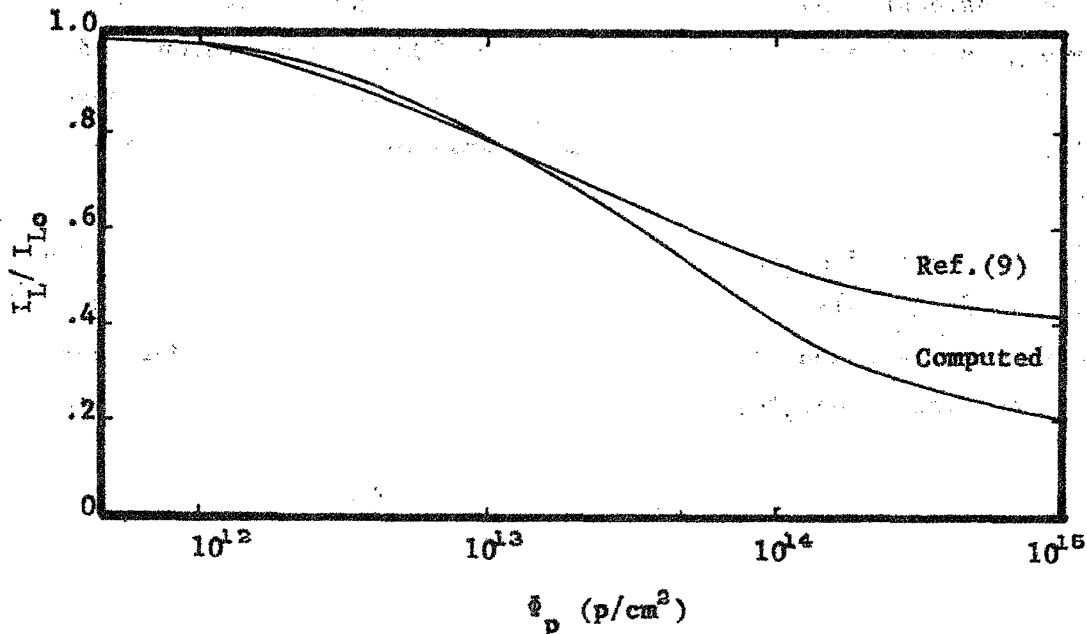

Figure 9. Degradation of I_L with 0.27 MeV protons

II. PROGRAM MODULE DESCRIPTIONS

The function of the solar cell program is twofold: 1) the determination of the solar cell parameters I_L and I_o; and 2) the associated I-V curve under various environmental conditions, including radiation damage by electron and proton spectra. The program is modular, i.e., a main program accompanied by several subroutines. The main program provides the data necessary to describe the solar cell and its environment, and calls the appropriate subroutine when needed. Each subroutine performs a specific task and is discussed individually below.

The environmental input consists of the temperature, the illumination intensity, and up to ten each of proton and electron energies with their associated fluences. Each fluence is considered to be incident isotropically. By suitable choices of energies and fluences,continuous particle spectra can be approximated. Particle energies are restricted to values below 200 MeV for protons and below 40 MeV for electrons. Particles with energies above these limits are ignored by the program because of lack of data on high energy damage coefficients.

A list of necessary input variables and their assumed values is given as Table 1. The values may be changed as desired, but care must be taken to retain the specified dimensions. More detailed discussions follow in the subroutine descriptions.

Table I. Input Variables for the Computer Program

Variable	Definition	Stored Value
XLO	initial base region minority carrier diffusion length	150 microns
D	base region minority carrier diffusion coefficient	35 cm^2/sec
RHO	base region resistivity	10 ohm-cm
VO	solar cell characteristic voltage	43 mv
R	solar cell series resistance	0.1 ohm
T	solar cell thickness	14 mils
XJU	junction depth	0.5 microns
CT	coverslide thickness	6 mils
TEMP	temperature	300 $^{\circ}K$
U	illumination intensity	140 mW/cm^2
EOP(I)	proton energies	0.0 MeV
PHP(I)	proton fluences	0.0 $protons/cm^2$
EOE(I)	electron energies	0.0 MeV
PHE(I)	electron fluences	0.0 $electrons/cm^2$
A(I)	absorption coefficients of light in silicon	variable: cm^{-1}
H(I)	spectral irradiances obtained from the Johnson spectrum	variable: $mW/cm^2-\mu$

A. Subroutine A B S C I S

Subroutine A B S C I S computes the increment thicknesses HX(K) necessary for the difference equation calculation, and the depth into the cell DX(K) of each corresponding point. The first 20 increments are of equal width delta; the remaining values of HX(K) are given by (K-20) delta. Therefore any error induced by the unequal increment technique occurs away from the junction. Such a compromise between equal and unequal increments reduces the degree of approximation in the critical region near the junction, resulting in a more accurate evaluation of the minority carrier concentration and, consequently, the photovoltaic current density.

The number of points is set at 200. Testing the program with a greater number of points (smaller increments) shows an insignificant change in the output.

B. Subroutine LIGHT

The rate of production of minority carriers per cm^3 per second due to light absorption is computed for each point provided by subroutine A B S C I S. A Simpson's rule integration over the Johnson spectrum from 0.4 to 1.1 microns in 0.05 micron steps is employed. Other spectra, e.g., the tungsten spectrum, may be used by changing the spectral irradiances H(I) in the subroutine's input data to those of the desired spectrum for the wavelengths 0.4, 0.45, ..., 1.1 microns.

C. Subroutine COVER

COVER approximates each monoenergetic isotropic proton fluence by a set of 50 beams incident at angles ranging from zero, with respect to normal incidence, to the maximum angle a proton of the given energy can have and still penetrate the coverslide and surface region. For each angle the proton energy after penetration

and the incremental fluence over the associated angular increment are determined. Computation terminates if the initial proton energy is insufficient to penetrate at normal incidence, or if the energy after penetration is insufficient to cause damage.

D. Subroutines PROTON and DAMAGE

Associated with each of the 50 beams determined by COVER is an angle dependent proton energy profile through the solar cell thickness. PROTON determines the energy at each point in the cell until such time as: 1) insufficient energy remains at a point DX(K) to penetrate the next increment HX(K); 2) the energy is below the damage threshold; or 3) the cell has been completely penetrated. It is assumed that the proton follows a straight path until one of the above conditions is met. To each of these energies subroutine DAMAGE associates a damage coefficient. These, in turn, are used with the incremental fluence to determine the degraded minority carrier diffusion length. A damaged diffusion length profile as a function of position in the cell results. Since the process is repeated for each beam of each energy the final diffusion length profile represents the total damage done by the approximated proton spectrum.

E. Subroutine ELECT

ELECT is the electron counterpart to subroutines COVER, PROTON, and DAMAGE. Here, however, the assumption of a non-deflected path cannot be made. We instead use a weighted damage coefficient to represent the damage at a given depth DX(K) in the cell, as described in the last quarterly report. The damage coefficient of the incident monoenergetic electron fluence is computed first. The effective damage coefficient at depth DX(K) is then determined as a function of the areal density in gm/cm^2 of material penetrated, i.e., DX(K)

plus the coverslide thickness. The coverslide and silicon densities are 2.2 and 2.33 gm/cm^3, respectively.

As in subroutine DAMAGE the minority carrier diffusion length profile is updated using the associated electron fluence and the weighted damage coefficients. The process is repeated for each electron energy given as input.

F. Subroutine ROOT

Subroutine ROOT contains the iteration technique to solve the difference equation. The value of the minority carrier concentration at the junction, C(1), is set equal to zero and an approximation of 10^8 made for its value at the second point C(2). The approximation of C(2) is then increased or decreased by an order of magnitude depending on the sign of the carrier concentration as computed for the back surface of the cell with the difference equation (Eq. 3). A positive sign results when C(2) is too large and a negative sign when it is too small. The process continues until the signs differ for two successive approximations, indicating that the correct value of C(2) lies between them. The bisection technique is then employed until either the carrier concentration at the back of the cell becomes zero, or two successive values of C(2) differ by less than 10^{-4} percent.

G. Subroutine TRAP

TRAP contains the actual difference equation approximation of the continuity equation. It is called by subroutine ROOT and control is returned if: 1) for a particular C(2), the minority carrier concentration anywhere in the cell exceeds 10^{30} $carriers/cm^3$; 2) the minority carrier concentration becomes negative; or 3) the computation for every incremental point is completed.

H. Subroutine CURVE

CURVE utilizes the previously determined data along with the input data to generate the photovoltaic current density I_L, the diode saturation current I_o, points on the resultant I-V curve, and their associated power P. The base region contribution to the photovoltaic current density is determined from the minority carrier concentration gradient at the junction, C(2)/HX(1). The surface region contribution is calculated from the junction depth, illumination intensity, temperature, and degraded minority carrier diffusion length at the junction (Eq. 13). Addition of the two current components yields the total photovoltaic current density. Temperature, illumination intensity, and degraded minority carrier diffusion length at the junction are used to approximate the diode saturation current.

A set of the four solar cell parameters is now available. The program is completed with the output of these parameters and points on the resultant I-V curve computed from the solar cell equation, and the power associated with each point. An example of the output is given in Table 2.

Table 2. Sample Printout of Solar Cell Performance

IL = 40.45

VO = 43.00

R = 0.100

IO = 0.176E-03

I	V	P
I = 0.00	V = 530.9	P = 0.00
I = 4.04	V = 525.9	P = 2.13
I = 8.09	V = 520.5	P = 4.21
I =12.13	V = 514.3	P = 6.24
I =16.18	V = 507.3	P = 8.21
I =20.22	V = 499.0	P =10.09
I =24.27	V = 489.0	P =11.87
I =28.31	V = 476.3	P =13.48
I =32.36	V = 458.4	P =14.83
I =36.40	V = 428.2	P =15.59
I =36.81	V = 423.7	P =15.59
I =37.21	V = 418.6	P =15.58
I =37.62	V = 412.8	P =15.53
I =38.02	V = 406.1	P =15.44
I =38.43	V = 398.2	P =15.30
I =38.83	V = 388.6	P =15.09
I =39.23	V = 376.2	P =14.76
I =39.64	V = 358.7	P =14.22
I =40.04	V = 328.9	P =13.17
I =40.45	V = 4.3	P = 0.17

III. CONCLUSIONS AND RECOMMENDATIONS

Although the primary objective during this quarter was to have the computer program operational (and this objective was reached), it is apparent from the preceding presentation that additional analysis was undertaken. This study was necessary for the model to take into proper account those significant variables discussed in Section I. The list of variables now considered, given by Table 1, is a measure of the present versatility of the program.

Even with additional analysis, there remain a number of variable factors affecting solar cell performance but not considered explicitly in the computer program. For example, we do not consider the surface and interface reflections of light, and overestimate photovoltaic current as a result. Partly, this is due to the lack of detailed reports on the commonly-used antireflective coatings; partly it is due to recognition that reflection is usually small. The same causes - paucity of data and low priority - have postponed our treatment of several factors. However, these may total to produce a significant effect.

To validate the program, it is therefore advisable to compare its output with specifically designed experiments. Such a validation effort would not only establish confidence in the computer results, but also would generate newer and more accurate measurements of those parameters now imperfectly measured, such as low energy proton damage coefficients, light absorption coefficients with varying temperature, etc. Meanwhile, the reasonable agreement of the computer results with published experiments, as shown in this and previous reports, warrants its use to evaluate existing and proposed solar cells.

IV. NEW TECHNOLOGY

After a diligent review of the work performed under this contract, it was determined that no new innovation, discovery, improvement or invention was developed.

REFERENCES

1. Smith, A. M.: Integrated Silicon Device Technology, Vol. IV----Diffusion. Tech. Doc. Report ASD-TDR-63-316, Volume IV. (AF 33(657)-10340; DDC no. AD 603716), Rearch Triangle Inst., Durham, N. C., Feb. 1964.

2. ARINC Research Corp.: Final Report on the Investigation of Factors Affecting Early Exploitation of Integrated Solid Circuitry. Tech. Doc. Report No. AFML-TR-64-385. (AF 33(657)-8785, Suppl. No. 3). Dec. 1964.

3. Conwell, E. M.: Properties of Silicon and Germanium, IRE, Proc. vol. 46, 1958. pp. 1281.

4. Macfarlane, G. C.; and Roberts, V.: Phys. Rev., vol. 97, pp. 1714, 1955; vol. 98, pp. 1865, 1955.

5. Newberger, M.: Silicon Data Sheets DS-137, May 1964 and Silicon Bibliographic Suppl. DS-137 Suppl., July 1968.

6. Morin, F. J.; and Maita, J. P.: Electrical Properties of Si Containing As and B. Phys. Rev., vol. 96, 1954, pp. 28.

7. Reynard, D. L.: Proton and Electron Irradiation of N/P Silicon Solar Cells. Report No. LMSC 3-56-65-4, Lockheed Aircraft Corp., April 1965.

8. Ritchie, D. W.; and Sandstrom, J. D.: Multikilowatt Solar Arrays. _In_ Sixth Photovoltaic Specialists Conf., Vol. II, March 1967, pp. 180-198.

9. Statler, R. L.; and Curtin, D. J.: Low Energy Proton Damage in Partially Shielded and Fully Shielded Silicon Solar Cells. Tech. Memo. CL-24-68, Communications Satellite Corp., Nov. 1968.